Ion-Specific Effects in the Colloid−Colloid or Protein−Protein Potential of Mean Force: Role of Salt−Macroion van der Waals Interactions

F. W. Tavares,[†] D. Bratko, H. W. Blanch, and J. M. Prausnitz*

Department of Chemical Engineering, University of California, Berkeley, California 94720, and Chemical Sciences Division, Lawrence Berkeley National Laboratory, Berkeley, California 94720

Received: December 11, 2003; In Final Form: March 31, 2004

In an aqueous electrolyte solution, the potential of mean force (PMF) for two macroions is affected not only by the size and charge of each electrolyte ion but also by the ion's polarizability. The Lifshitz theory provides a basis for calculating the van der Waals interaction between cation−colloid, anion−colloid, cation−cation, and anion−anion pairs. Monte Carlo simulations are used to determine how salt identity affects the PMF between colloidal particles or globular proteins in a saline solution, a phenomenon observed experimentally by Hofmeister for aqueous proteins more than 100 years ago. The calculations show that the PMF and, hence, solution phase behavior are sensitive to the van der Waals interaction between an ion and a macroion. The calculations described here may be useful for interpretation of experimental phase diagrams and for guiding design of separation processes where a salt is used to induce colloid or protein precipitation.

1. Introduction

For many years there has been much interest in the phase behavior of aqueous saline solutions of colloids or globular proteins. Aggregation of proteins is the probable cause of several neurological diseases, notably Alzheimer's disease,[1−4] and precipitation of a target protein from a multicomponent aqueous protein mixture is a common first step in purification of proteins in biotechnology.[5] Further, the stability of a colloidal solution is important in a variety of industries, notably in the production of inks and paints.[6]

A quantitative description of phase behavior in colloid solutions was presented more than 50 years ago in the form of the well-known DLVO theory.[7] That theory uses a potential of mean force (PMF) to describe the forces of repulsion and attraction between charged particles (macroions) suspended in a liquid, usually saline water. The DLVO PMF includes hard-sphere and electrostatic forces as well as (Hamaker) forces due to dispersion (van der Waals) attraction of two macroions.[7−9] An essential ingredient of the DLVO model and more advanced colloid theories is screening of electrostatic forces between the macroions.[7,10−13] However, the DLVO theory does not account for the effect of finite ion size on interaction among salt ions. Further, it considers only dispersion (van der Waals) pair potential *between the macroions* surrounded by the solvent, while it leaves out direct contribution from dispersion interactions of simple ions, and concomitant effects on electrostatic screening. Effects related to the molecular structure of the solvent and the intricate role of possible dissolved gas add further uncertainties[14] to predictions of DLVO theory. In addition to the simplifications of the physical model, the underlying Poisson−Boltzmann theory relies on a mean-field assumption[15] and hence neglects ion−ion correlations.[11,16,17] Such correlations can lead to qualitative deviations of DLVO predictions[17,18] from observed behavior.

Recent simulation calculations for the PMF (e.g., refs 17, 19−21) have taken into account the effect of correlations and ion size. These calculations show that for some cases, especially for solutions where the macroion's counterion is divalent, DLVO theory is not reliable.[17]

Published simulation calculations based on the conventional primitive model representation[17,19−21] cannot explain why two different salts with the same ionic valences and sizes exhibit different (often very different) effects on phase behavior of colloids or globular proteins as observed experimentally.[22−31] More than 100 years ago, Hofmeister reported that interprotein interactions are much more affected by some salts than by the others. The resulting Hofmeister series provides a qualitative indication of the salt effect on precipitation, as discussed in biochemistry textbooks. Dispersion forces related to ion polarizability, together with ion-specific solvation effects, have been identified[32] as a major cause of the observed behavior. Ninham and co-workers,[32−41] followed by others, have demonstrated that most specific ion effects can be explained theoretically by including ion−ion and ion−macroion dispersion forces[40−45] and ion hydration.[46,47]

In this work, we consider the effect of polarizable ions on the PMF between two globular macroions (colloids or proteins). We calculate the macroion−macroion PMF using Monte Carlo simulations, which incorporate excluded volume effects due to the finite size of the ions, as well as strong ion−ion correlations close to the macroions. We use the Lifshitz theory to calculate ion−ion and ion−macroion dispersion interactions; we then show how the mean force between two positively charged macroions varies with the type of anion for different sodium salts. The objective of our calculations is to estimate the magnitude of ion-specific effects on the intercolloidal PMF without invoking statistical mechanical approximations inherent to the Poisson−Boltzmann equation. Because the net ion-specific effect reflects an intricate interplay of direct dispersion interactions and their influence on electrostatic screening, it is desirable to minimize uncertainties due to the shortcomings of the mean field approach.

* Corresponding author. E-mail: prausnit@cchem.berkeley.edu.
[†] Permanent address: Escola de Química, Universidade Federal do Rio de Janeiro, Caixa Postal 68542, CEP 21949-900, Rio de Janeiro, RJ, Brazil.

10.1021/jp037809t CCC: $27.50
Published on Web 05/28/2004

For positively charged macroions, we consider monovalent counterions F^-, Cl^-, Br^-, I^-, $HCOO^-$, ClO_4^-, and NO_3^- and divalent counterions CO_3^{2-} and SO_4^{2-}. We also provide examples of ion identity effects on the mean force between two negatively charged macroions; results are presented for chloride salts with monovalent counterions Li^+, Na^+, K^+, Rb^+, and Cs^+ and divalent counterions Mg^{2+}, Ca^{2+}, Sr^{2+}, and Ba^{2+}.

2. Electrostatic and van der Waals Interactions

In the present study we focus on the contribution of ion−ion and ion−macroion van der Waals interactions to the colloid−colloid (or protein−protein) PMF. We adopt the primitive model where water is represented by a dielectric continuum; we defer to future studies specific solvation effects based on molecular representation of the solvent. At constant ionic strength and at constant macroion−macroion separations, the direct van der Waals interaction between two macroions (Hamaker force) is constant. Therefore, it is not included in the Hamiltonian that we use in simulations.

The interaction energy between particles i and j is the sum of three parts:

$$w_{ij} = w_{ij}^{hs} + w_{ij}^{elec} + w_{ij}^{disp} \quad (1)$$

The hard-sphere potential w_{ij}^{hs} is

$$w_{ij}^{hs} = \begin{cases} \infty & \text{for } r_{ij} < (\sigma_i + \sigma_j)/2 \\ 0 & \text{for } r_{ij} \geq (\sigma_i + \sigma_j)/2 \end{cases} \quad (2)$$

where r_{ij} is the center-to-center distance between particles i and j (ion or macroion). The electrostatic interaction w_{ij}^{elec} is

$$w_{ij}^{elec} = \frac{q_i q_j}{4\pi\epsilon_0\epsilon r_{ij}} \quad (3)$$

where q and σ are the charge and the diameter, respectively, of particle i (ion or macroion), $\epsilon_0 = 8.854 \times 10^{-12}$ C^2/(Jm) is the dielectric permittivity of vacuum, and ϵ is the dielectric constant of the solvent. Ignoring dielectric discontinuities in the solution,[48,49] we use a uniform dielectric constant $\epsilon = 78.5$, characteristic of water at 298 K.

Ion−Ion Dispersion Interactions. To calculate ion−ion dispersion interactions, we use the Lifshitz theory[8] for van der Waals forces. The dispersion potential w_{12}^{disp} between two small particles 1 and 2 (in this case, ions) in a medium 3 (the solvent) is given by:

$$w_{12}^{disp} = \frac{-B_{12}}{r_{12}^6} \quad \text{for} \quad r_{12} \geq (\sigma_1 + \sigma_2)/2 \quad (4)$$

The dispersion parameter B_{12} is calculated using multiple absorption frequencies:[42]

$$\frac{B_{12}}{k_B T} = 3\frac{\alpha_1(0)\alpha_2(0)}{[\epsilon_3(0)]^2} + \frac{3h}{\pi k_B T}\int_{\nu_{min}}^{\infty} \frac{\alpha_1(\nu)\alpha_2(\nu)}{[\epsilon_3(\nu)]^2}\, d\nu \quad (5)$$

where $\alpha_i(0)$and $\alpha_i(\nu)$ are the effective polarizabilities in water of particle i at frequencies 0 and ν, respectively, $\nu_{min} = 2\pi k_B T/h$ is the first nonzero frequency, $h\nu_{min} = 2.59 \times 10^{-13}$ erg at 298 K, where ν_3^I is the ionization frequency of the solvent and $h\nu_3^I = 20 \times 10^{-12}$ erg is the ionization energy of the solvent (water), h is Planck's constant, $\epsilon_3(\nu)$ is the dielectric constant of the solvent at frequency ν, and $\epsilon_3(0)$ is the static dielectric constant, i.e., the dielectric constant of the solvent (for water $\epsilon_3(0) = \epsilon = 78.5$). In eq 5, the first term on the right side represents the low-frequency contribution to the dispersion interaction and the second term represents the high-frequency contribution. For nonpolar molecules, the Clausius−Mossotti equation can be used to calculate $\alpha_i(\nu)$ in terms of $\epsilon_i(\nu)$, the dielectric constant of molecule i at frequency ν. However, because the dielectric constants of ions are unknown, we use eq 5 for calculation of the van der Waals dispersion interactions between ions.

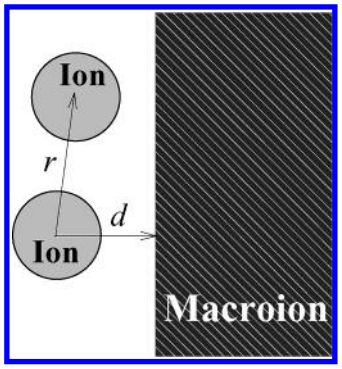

Figure 1. Schematic representation of a macroion and two small ions to calculate ion−ion and ion−macroion dispersion interactions. r is the center-to-center distance between two ionic species, and d is the perpendicular distance from the center of a small ion to the surface of a macroion.

Ion−Colloid Dispersion Interactions. To calculate ion−colloid dispersion interactions, we note that the ion is much smaller than the macroion; therefore, the ion−macroion van der Waals interaction is approximated by the potential between a small spherical particle i and a planar macroion m:[8]

$$w_{im}^{disp} = \frac{-B_{im}}{d_{im}^3} \quad \text{for} \quad d_{im} \geq \sigma_i/2 \quad (6)$$

where d_{im} is the perpendicular distance from the center of small particle i (ion) to the surface of macroion (colloid) m, as shown in Figure 1. The dispersion interaction parameter, B_{im}, is calculated from the Lifshitz theory:[32]

$$\frac{B_{im}}{k_B T} = \frac{\alpha_i(0)}{4\epsilon_3(0)}\left(\frac{\epsilon_m(0) - \epsilon_3(0)}{\epsilon_m(0) + \epsilon_3(0)}\right) + \frac{h}{4\pi k_B T}\int_{\nu_{min}}^{\infty} \frac{\alpha_i(\nu)}{\epsilon_3(\nu)}\left(\frac{\epsilon_m(\nu) - \epsilon_3(\nu)}{\epsilon_m(\nu) + \epsilon_3(\nu)}\right) d\nu \quad (7)$$

where $\epsilon_m(0)$and $\epsilon_m(\nu)$ are the dielectric constants of the macroion at frequencies 0 and ν, respectively.

To calculate dispersion interaction parameters, B_{ij} and B_{im}, we need to know how the effective polarizabilities of ions and the dielectric constants for the macroion and the solvent vary with frequency. For a molecule with one characteristic absorption frequency (the ionization frequency) ν^I, its polarizability and its dielectric constant at a frequency ν are given by the harmonic-oscillator model:[8,42,43,50]

$$\alpha(\nu) = \frac{\alpha(0)}{(1 + (\nu/\nu^I)^2)} \quad (8)$$

and

$$\epsilon(\nu) = 1 + \frac{(n^2 - 1)}{(1 + (\nu/\nu^I)^2)} \quad (9)$$

TABLE 1: Physical Properties for Water and Colloid or Protein

	water	colloid (protein)
refractive index (sodium D line) n	1.333	1.6[a]
dielectric constant $\epsilon(0)$	78.5	2.56[b]
ionization energy $h\nu^{I}$ (10^{12} erg)	20	20

[a] Suggested by Israelachvili[8] for proteins. [b] Obtained from $\epsilon(0) = n^2$ (Israelachvili[8]).

TABLE 2: Physical Properties of Ions

ion	polarizability in water[a] $\alpha(0)$ (Å^3)	free energy of hydration[b] ΔG_{hyd} (10^{12}erg)	ionization energy in a vacuum[c] $(h\nu^{I})^{V}$ (10^{12} erg)	ionization energy in water $h\nu^{I}$ (10^{12} erg)
Li^+	0.0285	−7.99	121.2	94.8
Na^+	0.1485	−6.23	75.76	54.7
K^+	0.7912	−5.05	50.68	33.1
Rb^+	1.3411	−4.67	43.72	27.3
Cs^+	2.2643	−4.28	37.10	21.9
Mg^{2+}	0.0720	−39.9	128.41	76.1
Ca^{2+}	0.4732	−30.5	81.57	41.0
Sr^{2+}	0.7706	−25.2	68.72	34.9
Ba^{2+}	1.4967	−23.0	60.9[d]	29.7
F^-	1.304	−7.84	5.449	10.9
Cl^-	3.764	−5.76	5.788	9.15
Br^-	5.068	−5.33	5.389	8.32
I^-	7.409	−4.70	4.898	7.19
NO_3^-	4.475	−5.10	6.277	8.97
ClO_4^-	5.453	−3.57	7.539	8.70
$HCOO^-$	4.208	−6.71	5.696	10.0
CO_3^{2-}	5.394	−7.95	−4.235	−0.673
SO_4^{2-}	6.327	−18.1	−27.57	−16.4

[a] From ref 53. [b] From Marcus.[55] [c] From CRC Handbook of Chemistry and Physics 83Rd (2002−2003) and from Marcus.[55] The anion ionization energy is obtained from its electron affinity. [d] Estimated using first, second, and third atomic ionization energies for Mg, Ca, Sr, and the first and second atomic ionization energies for Ba; from CRC Handbook of Chemistry and Physics 83Rd (2002−2003).

TABLE 3: Free Energy of Hydration Estimated Using Eq 15

	free energy of hydration (10^{12} erg)			
ion	(Marcus[55])	ion	(Marcus[55])	(calcd)
Ag^+	−7.307	Ag^{2+}	−30.82	−29.23
Cu^+	−8.884	Cu^{2+}	−33.48	−35.54
Fe^{2+}	−30.69	Fe^{3+}	−70.92	−69.05

where n is the refractive index for the sodium D line at 298 K. Equation 9 is used for both the solvent and for the macroion. As suggested by Ninham and Parsegian[51,52] and Ninham and Yaminsky,[32] eq 8 is also applied to cations and anions.

Equations 8 and 9 are substituted into eqs 5 and 7 to calculate the dispersion interactions between ion−ion and ion−macroion, respectively. Table 1 shows static dielectric constants, ionization energies and refractive indices for water and for colloid (or protein) taken from Israelachvili.[8] For cations and anions, Table 2 shows effective polarizabilities[53] and estimated ionization energies in aqueous solution as discussed in the next section.

The dispersion interaction parameters are obtained by integrating eqs 5 and 7 numerically, using the Romberg integration method.[54] Tables 4 and 5 give dispersion interactions at contact for ion−ion, eq 4, and ion−macroion, eq 6.

Ionization Energy. The ionization energy of a monovalent cation in a vacuum, say, Na^+, is obtained from the second atomic ionization energy; for a divalent cation, for example Ca^{2+}, it corresponds to the third atomic ionization energy. For an anion, say Cl^-, we use the electron affinity energy in a vacuum. These

TABLE 4: Nondimensional van der Waals Dispersion Interactions at the Contact Distance for Cation−Cation, Cation−Cl^-, and Cation−Macroion, in Water at 298 K[a]

cation	$\frac{B_{cation-cation}}{4096k_BT}$	$\frac{B_{cation-Cl^-}}{4096k_BT}$	$\frac{B_{cation-macroion}}{8k_BT}$
Li^+	0.00024	0.00341	0.0321
Na^+	0.0032	0.0160	0.138
K^+	0.0459	0.0741	0.574
Rb^+	0.1014	0.118	0.870
Cs^+	0.2139	0.182	1.273
Mg^{2+}	0.00117	0.00830	0.0758
Ca^{2+}	0.0220	0.0473	0.385
Sr^{2+}	0.0467	0.0733	0.575
Ba^{2+}	0.142	0.135	1.021

[a] For all cations and for Cl^-, $\sigma = 4$ Å. The ion−ion contact distance is $r = 4$ Å (eq 4) and $r^6 = 4096$ Å^6. The ion−macroion contact distance is $d = 2$ Å (eq 6) and $d^3 = 8$ Å^3.

TABLE 5: Nondimensional van der Waals Dispersion Interactions at the Contact Distance for Anion−Anion, Anion−Na^+, and Anion−Macroion, in Water at 298 K[a]

anion	$\frac{B_{anion-anion}}{4096k_BT}$	$\frac{B_{anion-Na^+}}{4096k_BT}$	$\frac{B_{anion-macroion}}{8k_BT}$
F^-	0.0291	0.00660	0.435
Cl^-	0.196	0.0160	1.086
Br^-	0.318	0.0194	1.348
I^-	0.573	0.0243	1.735
NO_3^-	0.271	0.0186	1.270
ClO_4^-	0.388	0.0219	1.508
$HCOO^-$	0.273	0.0196	1.310
CO_3^{2-}	0.0171	0.00129	0.112
SO_4^{2-}	1.146	0.0490	2.908

[a] For all anions and for Na^+, $\sigma = 4$ Å. The ion−ion contact distance is $r = 4$ Å (eq 4) and $r^6 = 4096$ Å^6. The ion−macroion contact distance is $d = 2$ Å (eq 6) and $d^3 = 8$ Å^3.

energies, presented in Table 2, are taken from the CRC Handbook of Chemistry and Physics, 83rd edition (2002−2003), and from Marcus.[55] However, for our purposes, we need ionization energies in water. The ionization energy in water is defined, for example, for Na^+ as the free energy change for the reaction:

$$Na^+(aq) \rightarrow Na^{2+}(aq) + e^-(aq) \tag{10}$$

A thermodynamic cycle can be used to calculate the free energy change in eq 10 provided that we know the changes in free energy for the following reactions:

$$Na^+(v) \rightarrow Na^{2+}(v) + e^-(v) \tag{11}$$

$$Na^+(v) \rightarrow Na^+(aq) \tag{12}$$

$$Na^{2+}(v) \rightarrow Na^{2+}(aq) \tag{13}$$

$$e^-(v) \rightarrow e^-(aq) \tag{14}$$

The free energy change for eq 11 is the ionization energy of Na^+ in a vacuum, given in Table 2. Equations 12−14 correspond to the process of hydration of Na^+, Na^{2+}, and electron, respectively. We know the hydration free energies of stable ions, for example, Na^+ (Table 2, from ref 55) and of an electron ($\Delta G_{hyd}^{(electron)} = -2.404 \times 10^{-12}$ erg, from ref 56). However, the hydration energies of unstable ions, e.g., Na^{2+}, are not available. Assuming that Born's equation[8] is sufficiently accurate to estimate hydration free energies of *both* the stable and unstable ionic species and that the size of the unstable ion (for example, Na^{2+}) is approximately the same as that of the stable ion (e.g.,

Na^+), the hydration free energy can be estimated from quadratic scaling with ion charge

$$\Delta G_{\mathrm{hyd}}^{(z\pm1)} = \left(\frac{z \pm 1}{z}\right)^2 \Delta G_{\mathrm{hyd}}^{(z)} \tag{15}$$

where $z + 1$ is the valence of the unstable cation and $z - 1$ is the valence of the unstable anion. This way, knowledge about hydration free energy for the stable species is exploited to estimate the corresponding value for the unstable species. Once determined, the hydration free energy is used to estimate the ionization potential of an ion in a solvent medium from the known value in a vacuum.

To test the accuracy of eq 15, we compare our hydration free energies with those of Marcus[55] for Ag^{2+}, Cu^{2+}, and Fe^{3+}, using the free energies for Ag^+, Cu^+, and Fe^{2+}, respectively. Table 3 shows that eq 15 provides hydration free energies within about 5%, sufficient for the purpose of the present study.

Table 2 gives estimated ionization energies for several cations and anions in water at 298 K.

3. Monte Carlo Simulation

Canonical Monte Carlo simulation is used to calculate the mean force $F(r)$ between two macroions in electrolyte solution at a given center-to-center distance r. Potential of mean force W is obtained by integration of the mean force:

$$W(r) = \int_{\infty}^{r} F(r)\, \mathrm{d}r$$

Details of calculating the PMF from the mean force are given elsewhere.[19,20]

In the Monte Carlo simulations, dispersion interactions of ion−ion and ion−macroion pairs are taken into account. The mean force between two macroion particles surrounded by small ions is the sum of four contributions:

$$F(r) = -\frac{\partial w_{\mathrm{mm}}^{\mathrm{elec}}}{\partial r} - \left\langle \sum_{i=1}^{N} \frac{\partial w_{\mathrm{im}}^{\mathrm{elec}}}{\partial r} \right\rangle - \left\langle \sum_{i=1}^{N} \frac{\partial w_{\mathrm{im}}^{\mathrm{disp}}}{\partial r} \right\rangle + F^{C}(r) \tag{16}$$

where the angular brackets denote canonical ensemble average, r is the center-to-center separation between two macroions. Subscript m denotes a macroion, superscript elec denotes electrostatic (Coulombic) forces, and superscript disp denotes van der Waals dispersion forces. The first term on the right-hand side of eq 16 is the direct Coulombic interaction between two macroions; this term is always repulsive for like-charged macroions. In eq 16, the term corresponding to the direct dispersion interaction (Hamaker forces) between two macroions is set equal to zero. The Hamaker term is independent of the other contributions and can be included or modified after calculation of all other terms is completed. The second term accounts for the Coulombic forces exerted on either of the macroions by all small ions. The third term accounts for the dispersion force exerted on either macroion by all small ions. The last term represents the mean force resulting from collisions between hard-sphere macroion particles and ions. The collision contribution to the mean force is calculated using a previously proposed procedure:[19,20]

$$F^{C}(r) = -k_{\mathrm{B}}T \lim_{\Delta r \to 0^+} \frac{\langle N_{\mathrm{C}} \rangle}{\Delta r} - k_{\mathrm{B}}T \lim_{\Delta r \to 0^-} \frac{\langle N_{\mathrm{C}} \rangle}{\Delta r} \tag{17}$$

Here, N_{C} is the number of salt ions that collide with the macroion because of a small variation of distance Δr. Equation 17 shows that the hard-sphere collision force is repulsive when small ions accumulate between the two macroions and is attractive when they are depleted.

Monte Carlo simulation details are reported elsewhere.[19,20] In summary, the cubic simulation box contains two identical macroion particles and 200 small ions that satisfy overall charge neutrality. The volume of the box is adjusted to give ionic strength 0.125 M. In all cases, the box length is about 1 order of magnitude larger than the Debye screening length; therefore, the electrostatic interaction between macroions due to the introduction of periodic boundary conditions is negligible. Standard canonical Monte Carlo simulation is applied to calculate the average forces and internal energies. During each run, the two macroion particles are fixed at a given separation distance, r, along the box diagonal, while the small ions are free to move throughout the box. The Ewald sum method is applied to account for long-range electrostatic interactions. Trial moves of macroion particles are used to determine collision probabilities. The limiting value of eq 17 is estimated by using a small but finite displacement Δr that yields an average collision probability for each trial move close to 10%.[20] For each macroion−macroion separation, 2×10^7 configurations are needed for equilibration. To calculate the average forces, 10^{10} configurations are used. The fluctuation in mean force is about 2%. The statistical uncertainty in the total internal energy is generally below 0.01%.

4. Results and Discussion

We have calculated the mean force between two macroions for systems that contain two identical macroions, with diameter $\sigma_{\mathrm{m}} = 20$ Å and valence +20, for cases where the counterions are anions and valence −20, when the counterions are cations. For all simulations, we use 200 small ions, all with the same diameter $\sigma_i = 4$ Å, such that we have charge neutrality. Therefore, for simulations containing a monovalent electrolyte, the number of counterions is 120 and the number of coions is 80. For simulations containing divalent counterions, the number of counterions is 80 and the number of co-ions is 120. The mean forces are normalized using the Bjerrum length, $l_{\mathrm{B}} = \mathrm{e}^2/(4\pi\epsilon_0\epsilon k_{\mathrm{B}}T)$, that represents the distance between two unit charges (e) where the pair potential equals thermal energy $k_{\mathrm{B}}T$. For all cases studied here, $T = 298$ K and $l_{\mathrm{B}} = 7.14$ Å.

Figure 2 shows the different contributions to the mean force between two macroions as a function of reduced intermacroion distance r/σ_{m} in a monovalent electrolyte solution of ionic strength 0.125 M. In this case, the counterions are anions; therefore, the simulation box contains 120 anions and 80 cations. Open circles represent electrostatic contributions to the inter-macroion mean force, solid triangles represent the collision contributions, and solid circles correspond to the van der Waals (dispersion) contributions. While Figure 2a is for a salt containing nonpolarizable (np) ions, i.e., without van der Waals interactions, Figure 2b is for NaI. Figure 3 shows the total mean forces obtained by the sum of collision, electrostatic, and van der Waals contributions where the open squares are for np and the solid squares are for polarizable NaI. The mean forces shown in these figures do not include the direct van der Waals interaction (Hamaker force) between two macroions.

For a nonpolarizable salt, shown in Figures 2a and 3, the total force, as well as its electrostatic and collision contributions, is repulsive at all distances. Also, both the collision and electrostatic interactions become insignificant at center-to-center

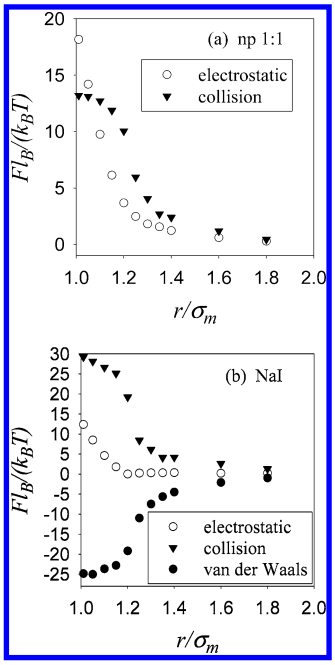

Figure 2. Contributions to the mean force (F) between two macroions in a monovalent electrolyte solution of ionic strength 0.125 M. (a) Salt with nonpolarizable (np) ions, i.e., without van der Waals interaction. (b) NaI. Open circles represent electrostatic contributions to the intermacroion mean force, solid triangles represent the collision contribution, and solid circles correspond to the van der Waals (dispersion) contribution.

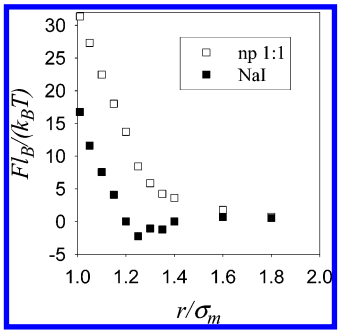

Figure 3. Total mean force between two macroions in a monovalent electrolyte solution of ionic strength 0.125 M for a salt with np ions and for NaI.

distances beyond about $1.8\sigma_m$. The electrostatic force decays monotonically with separation, as expected from DLVO theory. However, the overall hard-sphere collision force between charged colloids is quite different from that observed for uncharged systems. At short distances, the mean force between neutral colloids in a medium of neutral hard-sphere particles is generally attractive. However, for like-charged macroions dispersed in an electrolyte solution because of electrostatic attraction, the concentration of the counterions in the accessible region between adjacent macroions is much higher than that in the bulk solution and also exceeds the ion concentration at the macroion surface opposite the neighboring macroion particles. This effect is enhanced for polarizable ions as shown in Figures 2b and 3 for NaI. The attractive dispersion forces between the counterion (iodide) and the macroion increase the concentration of counterions around the macroion particles and consequently enhance both the hard-sphere repulsion and screening of the electrostatic forces. The electrostatic force decays quickly with distance and becomes insignificant at about $1.2\sigma_m$, a separation that is sufficient to accommodate a monolayer of counterions in between the macroions. At about the same distance, we also

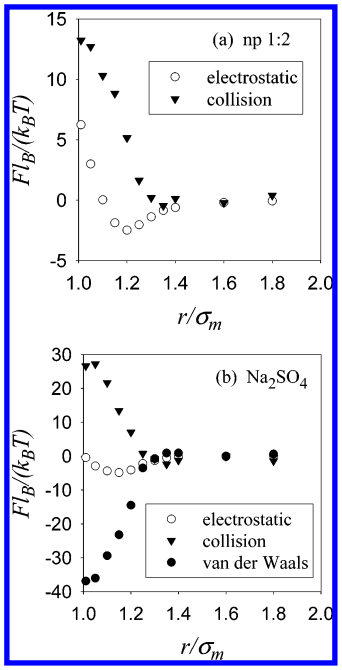

Figure 4. Contributions to the mean force between two macroions in a divalent electrolyte solution of ionic strength 0.125 M. (a) A salt with np ions. (b) Na_2SO_4.

observe rapid changes in the van der Waals and collision contributions to the mean force; these rapid changes are related to the accumulation of ions next to the macroion surface, here vaguely termed ion binding. In the polyelectrolyte and colloid literature, the term has frequently been used to describe ion localization within the ionic atmosphere of a macroion without requiring the action of specific short-ranged attraction.[57−61] In the present context, the term is used in a strictly qualitative sense and is intended to describe enhanced ion accumulation at the macroion surface due to attractive dispersion forces acting in concert with electrostatics. The additional ion binding provided by the van der Waals forces results in stronger screening of the electrostatic repulsion between equally charged macroions *and* provides a bridge of attraction between two macroions sharing common simple ions as their neighbors; hence, the simulated total force can be attractive at intermediate distances, as shown in Figure 3 for NaI.

Figure 4 shows different contributions to the mean force between two macroions at several intermacroion distances in a 1:2 electrolyte solution of ionic strength 0.125 M. The counterions are anions; therefore, the simulation box contains 80 divalent anions and 120 monovalent cations. While Figure 4a is for a salt containing np ions, Figure 4b is for Na_2SO_4. Open circles represent electrostatic contributions to the intermacroion mean force, solid triangles represent the collision contributions, and solid circles correspond to the van der Waals (dispersion) contributions. The total mean forces are presented in Figure 5 where the open squares are for nonpolarizable ions and solid squares are for Na_2SO_4. As for the previous cases, the mean forces shown in these figures do not include the direct van der Waals interaction (Hamaker force) between two macroions.

The mean forces obtained with divalent counterions indicate a behavior different from that with monovalent counterions. Even for nonpolarizable ions, an attractive force is observed within a range of small separations between the macroions. As indicated in Figures 4a and 5, for macroions near contact in the solution with nonpolarizable ions, the net force is strongly repulsive because of both electrostatic and hard-sphere interactions. The electrostatic force declines quickly with distance and

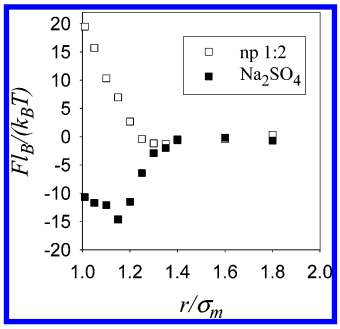

Figure 5. Total mean force between two macroions in a divalent electrolyte solution of ionic strength 0.125 M for salt with np ions and for Na_2SO_4.

reaches a negative minimum at about $1.2\sigma_m$. As the separation increases further, the force begins to decay and becomes insignificant. As pointed out elsewhere,[19−21,62] the attractive electrostatic force in solutions with nonpolarizable divalent counterions can be attributed to two effects: attraction from the intervening counterion layer and attraction due to the correlated density fluctuations in the double layers surrounding the two particles. While the same observations hold for solutions with monovalent counterions, the net force remains repulsive in that case because of a higher entropic penalty associated with localization of the screening monovalent counterions. Binding effects are enhanced for polarizable counterions as shown in Figures 4b and 5 for Na_2SO_4. Analogous to the system with monovalent counterions, the attractive dispersion forces between the counterion (sulfate) and the colloid lead to an increase in the concentration of counterions around the macroions and consequently enhance the hard-sphere repulsion *and* screening of electrostatic forces. The binding effect of sulfate is sufficient to make the electrostatic forces attractive, even at small separations. Therefore, the calculated total force is attractive at short distances, and the minimum is shifted to a shorter distance. While the neglect of structural solvation effects precludes quantitative comparisons with experiments, our results are consistent with industrial practice where ammonium sulfate is commonly used to induce protein precipitation.

The osmotic second virial coefficient (B) is frequently used to provide a measure of the strength of colloid−colloid (or protein−protein) interactions providing essential information about colloid−solution stability;[26,63] $B > 0$ indicates overall repulsive forces between two colloidal particles or protein molecules; the colloidal solution is then stable. However, $B < 0$ indicates overall intercolloid attraction, and the colloid (or protein) tends to precipitate. The virial coefficient is obtained by integration:[19,26]

$$B' = \frac{3B}{4\pi(\sigma_m + 2\delta)^3} = \frac{1}{2} + \int_{1+(2\delta/\sigma_m)}^{\infty} \left[1 - \exp\left(\frac{-W^p_{mm}}{k_BT}\right)\right] s^2 \, ds \quad (18)$$

where B' is the nondimensional osmotic second virial coefficient, $s = r/\sigma_m$ is the reduced distance, $\sigma_m + 2\delta$ is the effective diameter of a spherical colloidal particle (or protein), and δ is the thickness of the colloid's hydration layer. We use $\delta = 1.4$ Å as suggested by Norde.[64] This thickness is compatible with dynamic light-scattering measurements for lysozyme.[65] In eq 18, the first part of the right-hand side corresponds to the integration of hard-sphere interactions, and the second part is the contribution of the perturbation term of the PMF to B', where W^p_{mm} is the perturbation term of the PMF between two macroions. This perturbation term includes not only the electrostatic and indirect van der Waals interactions but also the direct van der Waals interaction (Hamaker force) between two macroions.

The direct van der Waals interaction (Hamaker force) between two macroions is given by:[6]

$$w^{disp}_{mm} = \frac{-H_{mm}}{12}\left\{\frac{\sigma_m^2}{r^2 - \sigma_m^2} + \frac{\sigma_m^2}{r^2} + 2\ln\left(1 - \frac{\sigma_m^2}{r^2}\right)\right\} \quad \text{for } r_{mm} > \sigma_m \quad (19)$$

where the Hamaker constant is calculated using Lifshitz's theory:[8]

$$\frac{H_{mm}}{k_BT} = \frac{3}{4}\left(\frac{\epsilon_m(0) - \epsilon_3(0)}{\epsilon_m(0) + \epsilon_3(0)}\right)^2 + \frac{3h}{4\pi k_BT}\int_{\nu_{min}}^{\infty}\left(\frac{\epsilon_m(\nu) - \epsilon_3(\nu)}{\epsilon_m(\nu) + \epsilon_3(\nu)}\right)^2 d\nu \quad (20)$$

Equation 9 is substituted into eq 20 to obtain the Hamaker constant by numerical integration, using the Romberg integration method.[54] We use the static dielectric constants, ionization energies, and refractive indices of water and macroion shown in Table 1. We obtain $H_{mm} = 4.96\ k_BT$, very close to that often used for proteins in aqueous solutions.[66,67]

According to the DLVO theory, the electrostatic part of the PMF is

$$(w^{elec}_{mm})^{DLVO} = \frac{z_m^2 l_B}{r_{mm}(1 + (k_D\sigma_m/2))^2}\exp[-k_D(r_{mm} - \sigma_m)] \text{ for } r_{mm} \geq \sigma_m \quad (21)$$

where k_D is the inverse Debye screening length, given by

$$k_D = \left(\frac{2e^2 N_A I}{\epsilon_0 \epsilon k_B T}\right)^{1/2} \quad (22)$$

where I is the ionic strength (here $I = 0.125$ M) and N_A is the Avogadro number.

To estimate the effects of taking into account the indirect van der Waals interactions (ion−ion and ion−colloid interactions) and the size of the ions, we compare the nondimensional osmotic second virial coefficient obtained by using the PMF from our Monte Carlo simulations with that from DLVO theory. In all cases, the ionic strength is 0.125 M and the direct van der Waals interaction (Hamaker force) (eq 19) is included. Results including direct and indirect dispersion and size effect are: $B' = 1.7$ for np 1:1, $B' = 0.84$ for NaI, $B' = -0.06$ for np 1:2, and $B' = -11$ for Na_2SO_4, while B' from DLVO theory equals 2.8, independent of the salt type. Despite the uncertainties unavoidable in simplified model estimates, these results show that the indirect van der Waals interactions (ion−ion and ion−macroion interactions) and ionic size are important for calculating thermodynamic properties of colloid and protein solutions.

To illustrate counterion specificity for a set of common ions, we calculate the total mean force between two macroions at $r = 1.3\sigma_m$ for solutions at ionic strength 0.125 M for different salts. The reference distance $r = 1.3\sigma_m$ is chosen in the range where ion-specific effects are still sufficiently strong, while minimizing the uncertainties due to neglect of molecular solvation (most significant in the macroion hydration shell).

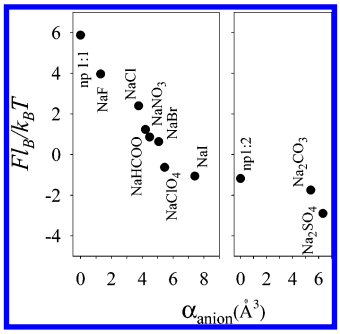

Figure 6. Effect of salt identity. Contributions to the total mean force between two macroions at $r = 1.3\sigma_m$ in a solution of ionic strength 0.125 M. The macroion net charge is +20. The counterions are anions. Raising ion polarizability and the valence of the counterion increases the attraction between two macroions.

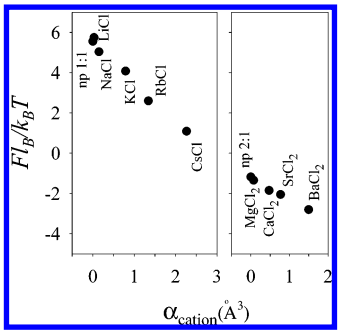

Figure 7. Effect of salt identity. Contributions to the total mean force between two macroions at $r = 1.3\sigma_m$ in a solution of ionic strength 0.125 M. The macroion net charge is −20. The counterions are cations. Raising ion polarizability and the valence of the counterion increases the attraction between two macroions.

Results do not include the direct macroion−macroion dispersion (Hamaker) force. Figure 6 presents results for monovalent salts NaF, NaCl, NaBr, NaI, $NaHCOO$, $NaClO_4$, and $NaNO_3$, and for divalent salts Na_2CO_3 and Na_2SO_4. The counterions are anions. The macroion net charge is +20.

The affinity of an anion for an anion-exchange resin depends on the resin employed, but the general trend[68] is given by the order $SO_4^{2-} > SCN^- > I^- > Br^- > Cl^-$. Figure 6 shows the same sequence, where the more negative the force, the higher the affinity of the anion-resin pair.

Figure 7 presents results for monovalent counterions Li^+, Na^+, K^+, Rb^+, and Cs^+, and divalent counterions Mg^{2+}, Ca^{2+}, Sr^{2+}, and Ba^{2+}. In this case, the macroion net charge is −20. Results do not include the direct macroion−macroion dispersion (Hamaker) force. In both figures, upon increasing the polarizability and the valence of the counterion, the attraction between two macroions increases. As reported by Everett,[69] the experimental effectiveness of monovalent cations in coagulating a negatively charged colloid usually varies in the order $Cs^+ > Rb^+ > K^+ > Na^+ > Li^+$; for divalent counterions, the order is $Ba^{2+} > Sr^{2+} > Ca^{2+} > Mg^{2+}$. The same sequence holds for ionic adsorption at surfaces, for ester hydrolysis, and for precipitation of albumin.[69] These experimental results agree with the sequence shown in Figure 7.

The magnitude of the salt-type contribution to the PMF depends on the ion−macroion dispersion interaction. Results presented in Figures 6 and 7 show that the mean force correlates well with the polarizability in water of the counterion that is directly related to ion−macroion dispersion interaction (Figure 8). However, the magnitude of the salt-type effect, i.e., the dispersion interaction between ion and macroion, is sensitive to the refractive index of the macroion. Figure 8 shows the effect

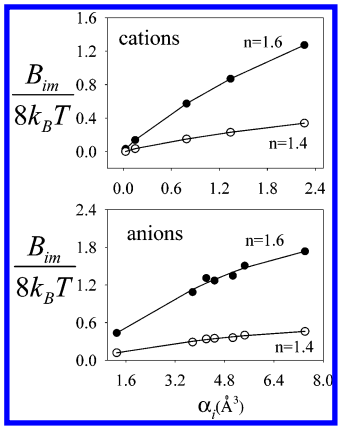

Figure 8. Effect of macroion's refractive index (n) on the nondimensional dispersion interaction at the contact distance for cation−macroion and for anion−macroion pairs. Solid circles represent ion−macroion dispersions for $n = 1.6$ and open circles are for $n = 1.4$. Monovalent cations, in order of polarizability, are Li^+, Na^+, K^+, Rb^+, and Cs^+. Monovalent anions, in order of polarizability, are F^-, Cl^-, $HCOO^-$, NO_3^-, Br^-, ClO_4^-, and I^-. Raising ion polarizability increases the ion−macroion dispersion interaction, but the ion identity effect is more important for macroions with higher refractive index.

of this refractive index (n) on the nondimensional dispersion interaction at the contact distance for cation−macroion and for anion−macroion pairs. Solid circles represent ion−macroion dispersions for a relatively high value $n = 1.6$, while open circles are for $n = 1.4$. Monovalent cations, in rising order of polarizability, are Li^+, Na^+, K^+, Rb^+, Cs^+. Monovalent anions, in rising order of polarizability, are F^-, Cl^-, $HCOO^-$, NO_3^-, Br^-, ClO_4^-, and I^-. Raising ion polarizability increases the ion−macroion dispersion interaction, but the ion identity effect is more important for a macroion with higher refractive index. Therefore, we expect that, for a colloid with low refractive index, the influence of van der Waals forces on ion identity is reduced.

While other effects, ignored in our simplified model, can influence the macroion−macroion interaction, a variety of observed phenomena, such as colloid and protein precipitation and ionic adsorption at surfaces, all related to salt specificity, can be interpreted along the lines indicated here. Without ruling out other important effects that may be responsible for the Hofmeister series, including those associated with molecular solvation, our calculations show that specific dispersion forces (van der Waals interactions) provide a significant part of the explanation of how the macroion−macroion potential of mean force depends not only on ionic size and charge but also on salt identity.

5. Conclusions

The mean force between two colloidal particles in a saline solution is calculated by augmenting electrostatic interactions with salt-specific dispersion (van der Waals) interactions between small ions and between small ions and macroions. The Lifshitz theory provides a basis for calculating the van der Waals interaction between macroion−macroion, cation−macroion, anion−macroion, cation−cation, and anion−anion pairs. Monte Carlo simulations are used to determine effects of salt identity on the intercolloidal potential of mean force in prototypical model systems. While our model relies on an approximate McMillan−Mayer representation of the solvent, the present results are qualitatively consistent with specific salt effects observed experimentally by numerous investigators, starting with Hofmeister for aqueous proteins more than 100 years ago. In agreement with earlier analyses by Ninham and co-workers, our

simulations indicate that the potential of mean force and, hence, the phase behavior of the colloidal or protein solution can be very sensitive to the van der Waals interaction that depends on salt identity. Specific dispersion forces between salt ions and ions and macroions, along with effects related to molecular solvation, may provide a key toward understanding salt-type effects as observed for colloidal and protein solutions.

Acknowledgment. We thank John Newman, Clay Radke, and Divesh Bhatt for discussions and Barry Ninham for his comments on the manuscript. For financial support, we are grateful to the Office of Basic Science of the U.S. Department of Energy and to the National Science Foundation through award BES 0118208. F.W.T. is grateful for financial support from CAPES/Brazil (Ministério da Educação) through grants BEX 0621/02-1.

References and Notes

(1) Pande, A.; Pande, J.; Asherie, N.; Lomakin, A.; Ogun, O.; King, J.; Benedek, G. B. *Proc. Natl. Acad. Sci. U.S.A.* **2001**, *98*, 6116.
(2) Serrano, M. D.; Galkin, O.; Yau, S. T.; Thomas, B. R.; Nagel, R. L.; Hirsch, R. E.; Vekilov, P. G. *J. Cryst. Growth* **2001**, *232*, 368.
(3) Booth, D. R.; Sunde, M.; Bellotti, V.; Robinson, C. V.; Hutchinson, W. L.; Fraser, P. E.; Hawkins, P. N.; Dobson, C. M.; Radford, S. E.; Blake, C. C. F.; Pepys, M. B. *Nature* **1997**, *385*, 787.
(4) Murphy, R. M.; Pallitto, M. R. *J. Struct. Biol.* **2000**, *130*, 109.
(5) Rothstein, F. *Differential Precipitation of Proteins, Cap 6 in Protein Purification Process Engineering*; Harrison, R. G., Ed.; Marcel Dekker: New York, 1994.
(6) Evans, D. F.; Wennerstrom, H. *The Colloidal Domain: Where Physics, Chemistry, Biology, and Technology Meet*, 2nd ed; VCH Publishers: New York, 1999.
(7) Vervey, J.; Overbeek, J. T. G. *Theory of the Stability of Lyophobic Colloids*; Elsevier: Amsterdam, 1948.
(8) Israelachvili, J. N. *Intermolecular and Surface Forces*; Academic Press: London, 1992.
(9) Mahanty, J.; Ninham, B. W. *Dispersion Forces*; Academic Press: London, 1976.
(10) Mitchell, D. J.; Ninham, B. W. *Chem. Phys. Lett.* **1978**, *53*, 397.
(11) Bratko, D.; Friedman, H. L.; Zhong, E. C. *J. Chem. Phys.* **1986**, *85*, 377.
(12) Nylander, T.; Kekicheff, P.; Ninham, B. W. *J. Colloid Interface Sci.* **1994**, *164*, 136.
(13) Kekicheff, P.; Ninham, B. W. *Europhys. Lett.* **1990**, *12*, 471.
(14) Alfridsson, M.; Ninham, B.; Wall, S. *Langmuir* **2000**, *16*, 10087.
(15) Barrat, J. L.; Hansen, J. P. *Basic Concepts for Simple and Complex Liquids*; University Press: Cambridge, 2003.
(16) Bratko, D.; Vlachy, V. *Chem. Phys. Lett.* **1982**, *90*, 434.
(17) Guldbrand, L.; Jonsson, B.; Wennerstrom, H.; Linse, P. *J. Chem. Phys.* **1984**, *80*, 2221.
(18) Kjellander, R.; Marcelja, S. *Chem. Phys. Lett.* **1984**, *112*, 49.
(19) Wu, J. Z.; Bratko, D.; Prausnitz, J. M. *Proc. Natl. Acad. Sci. U.S.A.* **1998**, *95*, 15169.
(20) Wu, J. Z.; Bratko, D.; Blanch, H. W.; Prausnitz, J. M. *J. Chem. Phys.* **1999**, *111*, 7084.
(21) Linse, P.; Lobaskin, V. *Phys. Rev. Lett.* **1999**, *83*, 4208.
(22) Taratuta, V. G.; Holschbach, A.; Thurston, G. M.; Blankschtein, D.; Benedek, G. B. *J. Phys. Chem.* **1990**, *94*, 2140.
(23) Baldwin, R. L. *Biophys. J.* **1996**, *71*, 2056.
(24) Melander, W.; Horvath, C. *Arch. Biochem. Biophys.* **1977**, *183*, 200.
(25) Curtis, R. A.; Prausnitz, J. M.; Blanch, H. W. *Biotechnol. Bioeng.* **1998**, *57*, 11.
(26) Curtis, R. A.; Ulrich, J.; Montaser, A.; Prausnitz, J. M.; Blanch, H. W. *Biotechnol. Bioeng.* **2002**, *79*, 367.
(27) Collins, K. D.; Washabaugh, M. W. *Q. Rev. Biophys.* **1985**, *18*, 323.
(28) Collins, K. D. *Biophys. J.* **1997**, *72*, 65.
(29) Collins, K. D. *Biophys. J.* **1999**, *76*, A127.
(30) Grigsby, J. J.; Blanch, H. W.; Prausnitz, J. M. *Biophys. Chem.* **2002**, *99*, 107.
(31) George, A.; Wilson, W. W. *Acta Crystallogr., Sect. D* **1994**, *50*, 361.
(32) Ninham, B. W.; Yaminsky, V. *Langmuir* **1997**, *13*, 2097.
(33) Bostrom, M.; Williams, D. R. M.; Ninham, B. W. *Langmuir* **2001**, *17*, 4475.
(34) Bostrom, M.; Williams, D. R. M.; Ninham, B. W. *Phys. Rev. Lett.* **2001**, *8716*.
(35) Bostrom, M.; Williams, D. R. M.; Ninham, B. W. *Langmuir* **2002**, *18*, 6010.
(36) Bostrom, M.; Williams, D. R. M.; Ninham, B. W. *J. Phys. Chem. B* **2002**, *106*, 7908.
(37) Bostrom, M.; Williams, D. R. M.; Ninham, B. W. *Langmuir* **2002**, *18*, 8609.
(38) Bostrom, M.; Williams, D. R. M.; Ninham, B. W. *Biophys. J.* **2003**, *85*, 686.
(39) Bostrom, M.; Craig, V. S. J.; Albion, R.; Williams, D. R. M.; Ninham, B. W. *J. Phys. Chem. B* **2003**, *107*, 2875.
(40) Pashley, R. M.; McGuiggan, P. M.; Ninham, B. W.; Brady, J.; Evans, D. F. *J. Phys. Chem.* **1986**, *90*, 1637.
(41) Dubois, M.; Zemb, T.; Fuller, N.; Rand, R. P.; Parsegian, V. A. *J. Chem. Phys.* **1998**, *108*, 7855.
(42) Netz, R. R. *Eur. Phys. J. E* **2001**, *5*, 189.
(43) Weissenborn, P. K.; Pugh, R. J. *J. Colloid Interface Sci.* **1996**, *184*, 550.
(44) Aveyard, R.; Saleem, S. M.; Heselden, R. *J. Chem. Soc., Faraday Trans. 1* **1977**, *73*, 84.
(45) Karraker, K. A.; Radke, C. J. *Adv. Colloid Interface Sci.* **2002**, *96*, 231.
(46) Manciu, M.; Ruckenstein, E. *Adv. Colloid Interface Sci.* **2003**, *105*, 63.
(47) Ruckenstein, E.; Manciu, M. *Adv. Colloid Interface Sci.* **2003**, *105*, 177.
(48) Bratko, D.; Jonsson, B.; Wennerstrom, H. *Chem. Phys. Lett.* **1986**, *128*, 449.
(49) Linse, P. *J. Phys. Chem.* **1986**, *90*, 6821.
(50) von Hipper, A. R. *Dielectric Materials and Applications*; John Wiley: New York, 1958.
(51) Ninham, B. W.; Parsegian, V. A. *Biophys. J.* **1970**, *10*, 646.
(52) Ninham, B. W.; Parsegian, V. A. *J. Chem. Phys.* **1970**, *53*, 3398.
(53) Pyper, N. C.; Pike, C. G.; Edwards, P. P. *Mol. Phys.* **1992**, *76*, 353.
(54) Press, W. H.; Teukolsky, S. A.; Vetterling, W. T.; Flami, B. P. *Numerical Recipes in FORTRAN: The Art of Scientific Computing*; University Press: Cambridge, 1992.
(55) Marcus, Y. *Ion Properties*; Marcel Dekker: New York, 1997.
(56) Zhan, C. G.; Dixon, D. A. *J. Phys. Chem. B* **2003**, *107*, 4403.
(57) Stigter, D. *J. Phys. Chem.* **1975**, *79*, 1015.
(58) Evans, D. F.; Mitchell, D. J.; Ninham, B. W. *J. Phys. Chem.* **1984**, *88*, 6344.
(59) Gunnarsson, G.; Jonsson, B.; Wennerstrom, H. *J. Phys. Chem.* **1980**, *84*, 3114.
(60) Mohanty, U.; Ninham, B. W.; Oppenheim, I. *Proc. Natl. Acad. Sci. U.S.A.* **1996**, *93*, 4342.
(61) Bratko, D.; Sheu, E. Y.; Chen, S. H. *Phys. Rev. A* **1987**, *35*, 4359.
(62) Hribar, B.; Vlachy, V. *J. Phys. Chem. B* **1997**, *101*, 3457.
(63) George, A.; Chiang, Y.; Guo, B.; Arabshahi, A.; Cai, Z.; Wilson, W. W. *Methods Enzymol.* **1997**, *276*, 100.
(64) Norde, W. *Colloids and Interfaces in Life Science*; Marcel Dekker: New York, 2003.
(65) Georgalis, Y.; Zouni, A.; Eberstein, W.; Saenger, W. *J. Cryst. Growth* **1993**, *126*, 245.
(66) Nir, S. *Prog. Surf. Sci.* **1977**, *8*, 1.
(67) Liu, W.; Bratko, D.; Prausnitz, J. M.; Blanch, H. W. *Biophys. Chem.* **2004**, *107*, 289.
(68) Gjerde, D. T.; Schmuckler, G.; Fritz, J. S. *J. Chromatogr.* **1980**, *187*, 35.
(69) Everett, D. H. *Basic Principles of Colloid Science*; The Royal Society of Chemistry: London, 1988.